Available online at www.sciencedirect.com
SCIENCE DIRECT
Catalysis Today 116 (2006) 433–438
CATALYSIS TODAY
www.elsevier.com/locate/cattod

Plate-like zinc oxide microcrystals: Synthesis and characterization of a material active toward hydrogen adsorption

D. Scarano [a,b,*], S. Bertarione [a,b], F. Cesano [a,b], J.G. Vitillo [a,b], A. Zecchina [a,b]

[a] *Department of Inorganic, Physical and Materials Chemistry, NIS (Nanostructured Interfaces and Surfaces) Centre of Excellence, University of Torino, Via P. Giuria 7, I-10125 Torino, Italy*
[b] *Consorzio INSTM (UdR of Torino), Italy*

Available online 5 July 2006

Abstract

ZnO-based materials have been synthesized by means of hydrothermal method from aqueous solutions of $ZnOH_4^{2-}$ in the presence of sodium-dodecyl sulphate (SDS). By means of a variety of analyses (SEM, AFM, IR, UV–vis and XRD) it is shown that this synthesis method allows to obtain ZnO microcrystals with well defined morphology and active toward hydrogen adsorption. The adsorption of hydrogen on these zinc oxide platelets has been investigated by FTIR spectroscopy and the results are compared with those obtained on ZnO, synthesized by combustion of zinc metal.

Keywords: Plate-like zinc oxide; Microcrystals; Hydrothermal synthesis; Hydrogen adsorption; XRD; Atomic force microscopy; Scanning electron microscopy; FTIR; UV–vis analyses

1. Introduction

In the last years, many studies have been focused both on the synthesis and the morphological–structural characterization of new functional materials. It is a wide spread opinion that to design the new generation of smart and functional materials, with specific properties [1,2], the control of size, shape and orientation of nano-/microcrystallites is an essential prerequisite.

ZnO is a challenging material with applications in many fields and has been synthesized under highly dispersed forms with various methods (sputtering, Zn combustion, CVD, etc.) [3–7]. Recently, synthetic techniques, based on solution chemistry or template methods, have been developed, which allow to modify the morphology and the particle size, by affecting diameters and aspect ratios [8–11]. Our interest in the synthesis of ZnO microcrystals with controlled morphology is motivated by the exceptional capacity of microcrystalline ZnO prepared by combustion of Zn to reversibly adsorb H_2 at RT [12,13]. The typical crystal habit of ZnO microcrystals prepared by combustion is prismatic and exhibits a low fraction of basal hexagonal planes (0 0 0 1) and (0 0 0 $\bar{1}$) and a predominant fraction of low-index unpolar (1 0 $\bar{1}$ 0) and (1 1 $\bar{2}$ 0) prismatic faces parallel to the *c*-axes. It is known that the 'low symmetry' unpolar faces can be easily cleaned from hydroxyl groups (adsorbed water) and are able to dissociate hydrogen at room temperature, with formation of Zn–H and O–H surface species [14–17]. The adsorption is fully reversible at room temperature. The polar hexagonal faces can be cleaned with difficulty from adsorbed water and are metastable [1]. A cooperative mechanism between adjacent surface Zn^{2+} and O^{2-} species has been hypothesized to explain the activity in hydrogen dissociation of the prismatic faces [16,17]. It must be underlined that the ability of prismatic faces to become covered by reversibly and dissociatively adsorbed H_2 at room temperature, makes ZnO unique among the oxidic systems (like MgO, Al_2O_3, SiO_2, etc.) [18–20] which are known to dissociate hydrogen only at rare defective sites [21]. It is known that the hydrogen dissociation is commonly observed on transition metal surfaces, where the mechanism is homolytic. The hydrogen dissociation on oxides occurs via the heterolytic splitting of H_2 on $M^{x+}O^{2-}$ pairs [22–24].

* Corresponding author at: Department of Inorganic, Physical and Materials Chemistry, University of Torino, Via P. Giuria 7, I-10125 Torino, Italy. Tel.: +39 011 6707834; fax: +39 011 6707855.
E-mail addresses: domenica.scarano@unito.it (D. Scarano), serena.bertarione@unito.it (S. Bertarione), federico.cesano@unito.it (F. Cesano), jenny.vitillo@unito.it (J.G. Vitillo), adriano.zecchina@unito.it (A. Zecchina).

0920-5861/$ – see front matter
doi:10.1016/j.cattod.2006.05.062

Otherwise $M^{x+}O^{2-}$ pairs, sufficiently 'reactive' in hydrogen splitting, are rare and the reaction occurs on defective sites. ZnO is the only oxidic system, where the splitting is involving extended faces, with formation of ZnH and OH pairs. Another relevant characteristic is the reversibility of the process at room temperature. This means that dissociated H^+ and H^- fragments are prone to participate to hydrogenation reaction as reported by Chang and Kokes [25], Kokes et al. [26] and Dent and Kokes [27]. It is noteworthy that such ability of ZnO system is helping to explain the chemical activity of Cu/ZnO systems in industrial synthesis processes [28,29].

Unfortunately, the low surface area of ZnO prepared by Zn combustion (about 10 $m^2\ g^{-1}$) does not allow to reach a reasonable H/ZnO ratio, which is the only factor which can make ZnO/H_2 system interesting not only for catalytic purposes but also for hydrogen storage. In order to increase the adsorption properties, many efforts have been made in our laboratory to produce high surface area ZnO-based materials. These efforts included the systematic investigation of ZnO samples obtained from thermal decomposition of: (i) oxalate, (ii) citrate, (iii) carbonate and (iv) hydroxide both pure and SiO_2 supported. Although these materials have surface area much higher than that of ZnO obtained by combustion, they prove ineffective in hydrogen adsorption, probably because of their ill defined morphology and associated negligible proportion of prismatic faces. Recently, the publication of a novel method for the synthesis of microcrystalline ZnO with defined morphology [30] has renewed our interest in the ZnO/H_2 system. In this communication, we discuss about the morphology and surface properties of ZnO microcrystals prepared following a variant of the recently published method [30]. By means of a variety of analyses (SEM, AFM, IR, UV–vis and XRD) it will be shown that this synthesis variant allows to affect the morphological properties of ZnO microcrystals in such a way to promote promising properties for hydrogen adsorption.

2. Experimental

Microcrystalline ZnO samples have been synthesized by means of a modified process in solution at room temperature and at atmospheric pressure derived from Ref. [30]. An aqueous solution of 20 ml of $ZnCl_2$ [1 M] is added to 45 ml deionized H_2O under stirring at room temperature into a flask. Then 30 ml of NaOH [4 M] aqueous solutions and 5 ml of sodium-dodecyl sulphate (SDS) [0.1 M] were added dropwise to the $ZnCl_2$ solution. The flask was then closed and heated at 60 °C for 1.5 h and at 80 °C for 2 h. Then the solution was cooled at room temperature and aged for 2 days under vigorous stirring. Finally, the solution was heated again at about 90–95 °C for 2 h and the resulting powder was collected, thoroughly washed with deionized water and dried at 85 °C for 3 h. The obtained material has a surface area of 31 $m^2\ g^{-1}$, as determined by N_2 adsorption at 77 K (BET method). The surface properties of this sample were compared with those of ZnO obtained by combustion (Kadox 25, New Jersey Zinc Co., BET surface area: 10 $m^2\ g^{-1}$).

Crystal structure and phase identification of the materials have been performed by XRD analyses by Philips PW3020 X-ray diffractometer operating with Cu Kα radiation in a Bragg Brentano configuration. The observed patterns have been analysed using Philips X'Pert HighScore software and compared with standard patterns of International Centre of Diffraction Data (ICDD) and powder diffraction file (PDF) databases.

The microcrystals morphology has been investigated by means of 420 Stereoscan SEM apparatus, equipped with Oxford EDS system and by means of atomic force microscopy AFM, on a Park Scientific Instrument Auto Probe LS. Large scale images are obtained in contact mode regime, using microlevers sharpened silicon nitride pyramidal tips with a radius of curvature less than 200 Å (cantilever thickness = 0.6 μm; cantilever width = 18 μm; cantilever length = 180 μm; force constant = 0.05 N m^{-1}; resonant frequency = 22 kHz). The AFM images were recorded in air at room temperature.

Diffuse reflectance UV–vis spectra were also recorded at RT on both samples, by means of a Varian Cary 5 spectrometer.

For infrared studies, thin self-supported pellets of both ZnO samples were prepared and activated by outgassing at 773 K for 1 h under a dynamic vacuum (residual pressure 10^{-4} Torr) inside an IR cell, which also allowed gas dosage and low temperature IR measurements to be carried out. In order to compensate for the oxygen loss during thermal activation of the pellets (which makes the samples non-stoichiometric and non-transparent in the IR region), at the end of the activation period, 20 Torr of oxygen was dosed to the sample (still kept at 773 K). Then the sample was cooled to room temperature and oxygen removed by outgassing at room temperature to a final pressure of 10^{-4} Torr.

On the so treated samples, the IR spectra of H_2 adsorbed at room temperature and of CO adsorbed at liquid N_2 temperature were obtained. The FTIR spectra were recorded in situ at 2 cm^{-1} resolution, using a Bruker IFS 28 spectrometer, equipped with a cryogenic MCT detector.

3. Results and discussion

3.1. Structure and morphology

To verify the cristallinity of the as-synthesized samples, the XRD pattern (Fig. 1a) is compared to that of ZnO obtained by burning Zn powders in oxygen (Kadox ZnO) [31,32] (Fig. 1b) and to that of standard Zincite (CAS no. 00-036-1451), used as reference (Fig. 1c).

From Fig. 1 the following considerations can be derived. (i) The XRD pattern of samples obtained by the hydrothermal method is well defined (Fig. 1a), indicating that ZnO crystalline structures are formed. (ii) The broader character of the diffraction peaks with respect to ZnO sample obtained by combustion is suggestive of a smaller average crystal size. (iii) Considering this pattern in more detail, it can be observed that it exhibits an intensity ratio for the (1 0 0) and (0 0 2) reflections different from that of Kadox ZnO. This means that the

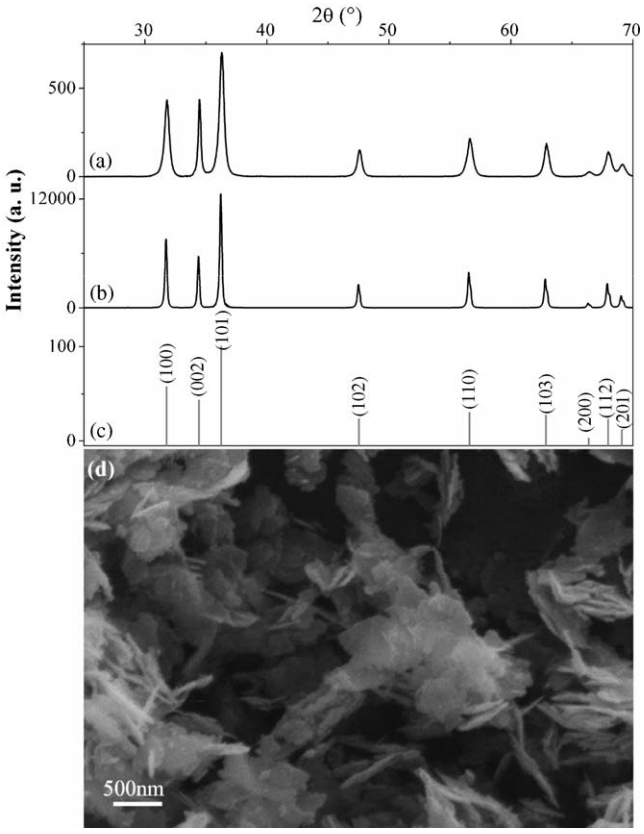

Fig. 1. XRD patterns of plate-like ZnO particles (a), Kadox ZnO (b) and Zincite (c) and SEM image of plate-like ZnO particles (d).

directional growth of the crystallites along the *c*- and *a*-axes occurs in different proportion in the two samples.

The morphology of a dense aggregate as obtained by SEM is imaged in Fig. 1d. From this figure, it is clear that the crystallites have the shape of very thin platelets, whose typical diameter appears in the 0.5–1.0 μm range at this level of magnification. The individual platelets and the platelets aggregates are randomly oriented with respect to the deposition plate. In comparison with the crystals of Kadox ZnO, characterized by elongated prismatic habit (*images not reported for sake of brevity*) [31,34], these ZnO microcrystals have distinctly different habit. On the basis of the SEM images it is not possible to infer about the index of the most exposed faces responsible for the platelet form of the microcrystals.

Further details on the microcrystals morphologies come from large area AFM images (Fig. 2). In this figure, the three-dimensional views of two different regions, with sizes comprised in the 0.1–0.5 μm range, are imaged (Fig. 2a and b).

On the basis of these figures, the presence of layered and packed platelets with hexagonal shape is evident, indicating that hexagonal planes are predominant and are responsible for the shape of the microcrystals (Fig. 2b). This is certainly related to the function of the capping agent (sodium-dodecyl sulphate), which partially inhibits the growth along the prismatic faces and promotes the preferential growth of basal planes with the formation of platelets [33–37].

From the height profiles, large terraces and steps, running along well defined directions are also well evident. The terraces

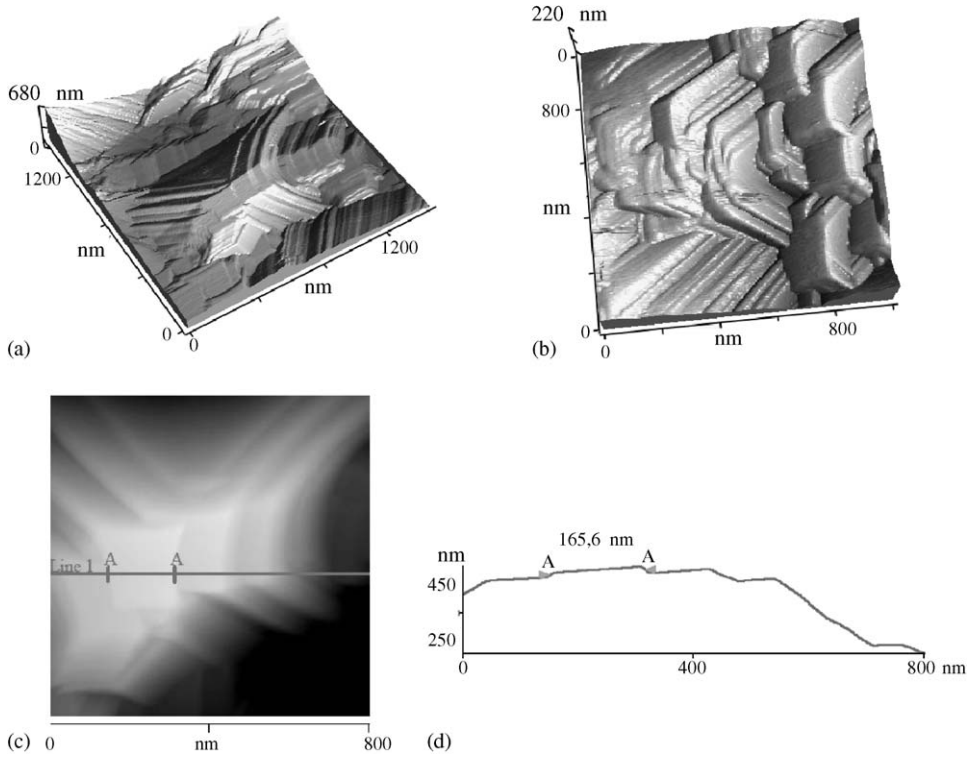

Fig. 2. Large scale *contact*-AFM (1.5 μm × 1.5 μm (a), 1 μm × 1 μm (b) and 0.8 μm × 0.8 μm (c)) topographies of ZnO crystallites on three different areas of the sample. (d) The height profile, measured across the grey line on the (c) image, is reported.

(prismatic faces) appear highly regular and defects free, at least at macroscopic level. It is noteworthy that the average height of prismatic faces can be evaluated less than 200 nm (Fig. 2d), being this value a definitely small figure with respect to that observed for the hexagonal faces. In conclusion, AFM images are consistent with aggregates of packed particles with approximately hexagonal shape exhibiting both basal and prismatic faces. Contrary to ZnO oxide, obtained by combustion, basal faces are present in larger proportion.

The different morphology and shape of plate-like particles is influencing also the optical properties as demonstrated by UV–vis spectra (Fig. 3). As a matter of fact plate-like particles are characterized by an absorption edge located at a slightly higher frequency value with respect to that of Kadox ZnO (in agreement with the larger dimensions of the ZnO microcrystals, produced by Zn combustion) [31].

3.2. FTIR spectra of CO and H_2 adsorbed on plate-like and Kadox ZnO

The results presented so far give only a macroscopic information about the microcrystals shape and morphology. Consequently at this stage nothing is known about the structure at the atomic level of the exposed surfaces. This difficulty can be partially overcome by means of the method of the probe molecules. As a matter of fact it has been demonstrated in Refs. [16,31,32], that the structure of the surfaces at the atomic level can be investigated by studying the IR spectroscopy of adsorbed probe molecules. For instance, it is known that the vibrational spectroscopy of adsorbed CO is influenced by: (i) the index, (ii) the extension, (iii) the defective character of the adsorbing planes and (iv) the presence of adsorbates.

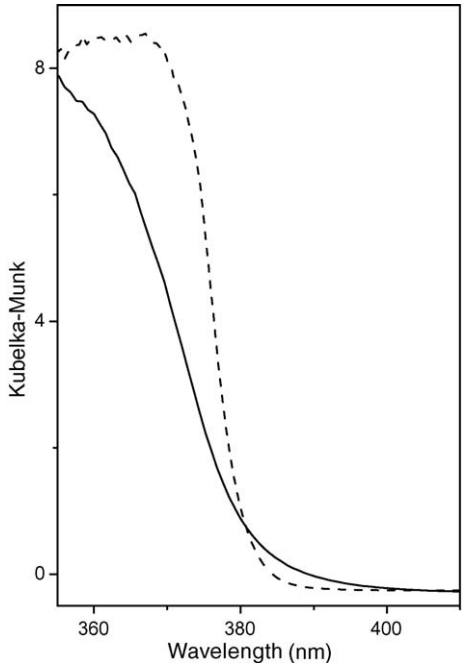

Fig. 3. UV–vis spectra of plate-like ZnO particles (solid line) and Kadox ZnO (dashed line) at 298 K.

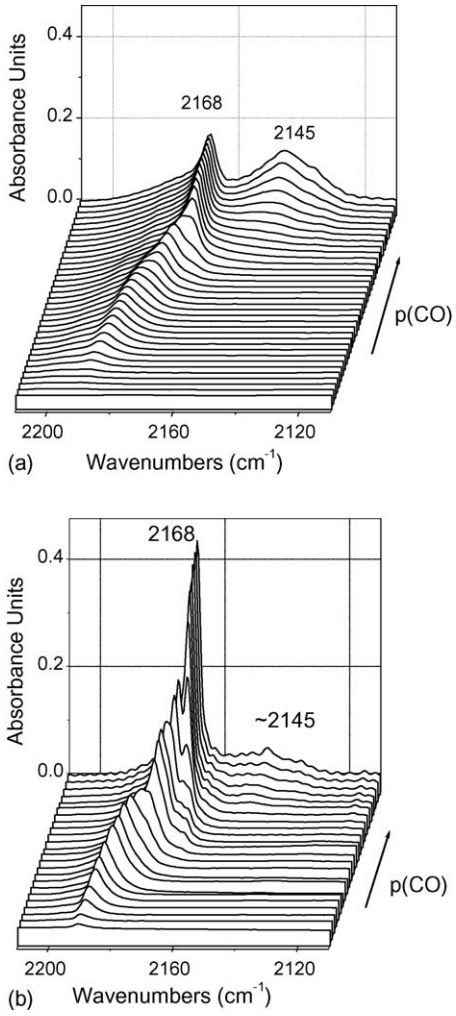

Fig. 4. FTIR spectra of CO adsorbed at 77 K on (a) plate-like ZnO and (b) Kadox ZnO samples, by decreasing progressively the coverage (θ_{max} p(CO) = 2.66 kPa; θ_{min} p(CO) → 0).

For this reason we have investigated the surface structure of ZnO, prepared as described before, by means of IR spectroscopy of adsorbed CO. The results, reported in Fig. 4a (platelets) are compared with those obtained on Kadox ZnO (Fig. 4b). In this figure, the two sequences of spectra obtained at liquid nitrogen temperature and corresponding to surface coverage ranging in the θ = 0–1 interval are illustrated. In both cases, the samples were previously outgassed at 773 K under vacuum, which is a temperature treatment sufficient to clean the prismatic faces from hydroxyl groups, which so expose an ordered array of coordinatively unsaturated Zn^{2+} ions. Otherwise this thermal treatment is not sufficient to clean the remaining terminations, which so are covered by hydroxyl groups. As the spectroscopy of CO on Kadox ZnO is well understood, it is useful to discuss at first the spectra reported in Fig. 4b. The IR bands can be divided into two groups; those located in the 2200–2160 cm^{-1} interval and those occurring in the 2160–2120 cm^{-1} interval (with an apparent maximum at 2145 cm^{-1}).

The bands located in the 2200–2160 cm^{-1} interval are due to CO adsorbed on Zn^{2+} ions on the (1 0 $\bar{1}$ 0) and (1 1 $\bar{2}$ 0) faces.

The continuous shift with the coverage of the CO peak, initially observed at 2190 cm^{-1} ($\theta \rightarrow 0$), is due to the progressive building up of lateral interactions between the parallel CO oscillators adsorbed on an ordered array of Zn^{2+} centres. This is a well known phenomenon and will not be further commented [31]. We only remark that on Kadox ZnO at full coverage ($\theta = 1$, at 77 K and 2.66 kPa) all the vacant sites are filled and the prismatic faces can be considered as fully covered by CO, with no adjacent vacant sites. This model is able to explain also the gradual decrease of the half-width of the band when $\theta \rightarrow 1$. In fact, as θ changes from 0 to 1, the disorder in the surface adlayer decreases progressively and at $\theta = 1$ the surface phase is fully ordered (one CO per Zn^{2+} ion) [31]. The broad feature at 2145 cm^{-1} is due to CO adsorbed on OH covered surfaces (i.e. the non-prismatic ones including the basal ones, etc.).

When the sequence of spectra on plate-like ZnO is considered (Fig. 4a), it comes out: (i) the relative intensity of the absorptions in the 2200–2160 and 2160–2120 cm^{-1} ranges indicates that extension of prismatic faces is smaller with respect to Kadox ZnO, while the proportion of hydroxilated faces has increased: this result fully confirms the observation obtained by XRD, SEM and AFM analyses; (ii) the bands in the 2200–2160 cm^{-1} range undergo a continuous shift with coverage similar to that found on Kadox ZnO: this implies that the array of Zn^{2+} ions on exposed prismatic faces is well ordered and in this case too their surface can be considered as fully covered by CO, as we infer from the invariance at the highest coverage of the intensity of the 2168 cm^{-1} peak; (iii) the half-width of the bands in the 2200–2160 cm^{-1} interval is larger on platelets than on Kadox ZnO: this is likely related to the smaller size of the prismatic faces present on platelets (in agreement with the SEM and AFM results).

The adsorptive ability toward hydrogen of zinc oxide platelets has been investigated by FTIR spectroscopy and the results are compared with those obtained on Kadox ZnO, obtained by combustion of zinc metal [31,32].

Fig. 5a shows the FTIR spectra obtained after adsorption of H_2 at 298 K at increasing coverage, on ZnO plates, while Fig. 5b shows a similar sequence of spectra obtained on Kadox ZnO. These spectra, which depict the characteristic features already reported and thoroughly discussed in the literature [16,17], are shown here for the main purpose of investigating the hydrogen adsorption ability of these systems.

Briefly, both sequences of spectra in Fig. 5a and b show two IR absorptions in the 1710–1707 and 3506–3490 cm^{-1} intervals which correspond, respectively, to the fundamental stretching vibrations of hydride (Zn–H) and hydroxyl (O–H) surface species, formed upon dissociative chemisorption of the dihydrogen molecule on adjacent $Zn^{2+}O^{2-}$ ion pairs of prismatic faces (behaving as Lewis acid–base couples). The coordinatively unsaturated ZnO pairs on the prismatic faces are all structurally equivalent [16]. It has been shown that the presence of Zn–H and O–H groups formed by dissociative adsorption of hydrogen creates repulsive forces that limit further hydrogen adsorption, thus leaving a fraction of the Zn sites unoccupied [16,27]. In particular, it has been shown by Dent and Kokes [27] that the saturation coverage on Kadox

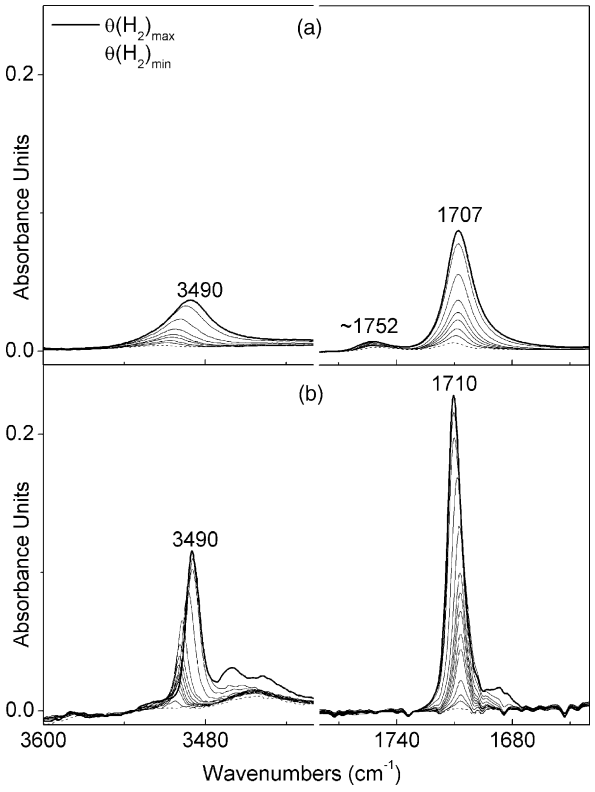

Fig. 5. FTIR spectra of H_2 adsorbed at 298 K on plate-like ZnO (a) and Kadox ZnO (b) samples by decreasing progressively the coverage (θ_{max} $p(H_2) = 16$ kPa; θ_{min} $p(H_2) \rightarrow 0$): O–H species (on the left side) and Zn–H species (on the right side) absorption regions.

ZnO (reached at RT at about 5.2 kPa) corresponds to about 5% of the monolayer, which accounts for a H/Zn ratio of ~0.5 on the prismatic faces [16]. As a matter of fact, on the basis of previous papers [16,17] it comes out that adsorption of CO on H_2 precovered-ZnO samples is partially inhibited, as only a small portion of sites is available for adsorption of new incoming molecules.

The bands undergo a gradual and opposite shift with coverage. This coverage dependent frequency shift of the Zn–H and O–H stretching bands has been explained in the past [16,17] in terms of lateral interactions among neighbouring molecules adsorbed in ordered arrays like those present on facelets and terraces. These lateral effects are similar (although smaller) to those observed with CO. Other minor features at 1752 and 3605 cm^{-1} (the last one not shown in the figure) are observed, which can be assigned to Zn–H and O–H species adsorbed on more defective situations. We only remark that dissociative chemisorption of the dihydrogen molecule takes place in a reversible way and that this fact is supporting the possibility to perform fully reversible adsorption and release cycles at room temperature, which means that every subsequent hydrogen dosage on the same system results in equivalent performances, not requiring pretreatments between cycles [27].

The comparison of the two sequences of FTIR spectra (Fig. 5a and b) also suggests that the ZnO plates are characterized by a smaller extension of the surfaces involved

in the hydrogen chemisorption process, with respect to Kadox ZnO, being this result parallel to that obtained with CO. Moreover the higher values of the half-width of IR peaks associated with the Zn–H and O–H species on the platelets are indicative of a lower level of regularity associated with the reduced extension of the prismatic terraces and then with a reduced ability toward hydrogen adsorption as compared to Kadox ZnO.

4. Conclusions

In this contribution, it is shown that a simple method, based on a low temperature synthesis in solution, gives ZnO materials having surface area larger than Kadox, which are able to dissociate hydrogen. This result is remarkable since ZnO samples obtained by traditional methods like carbonate, oxalate and hydroxide decomposition, did not show a sufficient activity toward hydrogen adsorption. This result also shows that the ability to reversibly adsorb H_2 at room temperature is not only a property of ZnO obtained by combustion of Zn, and that ZnO obtained through synthetic methods under mild conditions, can give encouraging results.

Acknowledgements

This work was supported by MIUR, INSTM Consorzio and NIS (Nanostructured Interfaces and Surfaces) Centre of Excellence.

References

[1] L. Vayssieres, K. Keis, A. Hagfeldt, S.E. Lindquist, Chem. Mater. 13 (2001) 4395.
[2] M.S. Gudiksen, J. Wang, C.M. Lieber, J. Phys. Chem. B 105 (2001) 4062.
[3] Z.L. Wang, Mater. Today 7 (2004) 26.
[4] M.H. Huang, Y.L. Wu, H. Feick, N. Tran, E. Weber, P. Yang, Adv. Mater. 13 (2001) 113.
[5] X. Wang, C.J. Summers, Z.L. Wang, Adv. Mater. 16 (2004) 1215.
[6] X. Wang, Y. Ding, C.J. Summers, Z.L. Wang, J. Phys. Chem. B 108 (2004) 8773.
[7] Q. Wan, C.L. Lin, T.H. Wang, Appl. Phys. Lett. 84 (2004) 124.
[8] H.G. Yang, H.C. Zeng, J. Am. Chem. Soc. 127 (2005) 270.
[9] H. Yu, Z. Zhang, M. Han, X. Hao, F. Zhu, J. Am. Chem. Soc. 127 (2005) 2378.
[10] B. Liu, H.C. Zeng, J. Am. Chem. Soc. 126 (2004) 16744.
[11] A. Taubert, G. Glasser, D. Palms, Langmuir 18 (2002) 4488.
[12] G. Hussain, N.J. Sheppard, J. Chem. Soc. Faraday Trans. 86 (1990) 1615.
[13] G. Ghiotti, A. Chiorino, F. Boccuzzi, Surf. Sci. 287/288 (1993) 228.
[14] A. Wander, N.M. Harrison, J. Phys. Chem. B 105 (2001) 6191.
[15] E.V. Lavrov, J. Weber, F. Borrnert, C.G. Van de Walle, R. Helbig, Phys. Rev. B 66 (2002) 65205.
[16] A. Zecchina, D. Scarano, S. Bordiga, G. Spoto, C. Lamberti, Adv. Catal. 46 (2001) 265.
[17] D. Scarano, S. Bertarione, G. Spoto, A. Zecchina, C. Otero Areán, Thin Solid Films 400 (2001) 50.
[18] D. Scarano, S. Bordiga, S. Bertarione, G. Ricchiardi, A. Zecchina, Catal. Lett. 68 (2000) 185.
[19] E.N. Gribov, S. Bertarione, D. Scarano, C. Lamberti, G. Spoto, A. Zecchina, J. Phys. Chem. B 108 (2004) 16174.
[20] G. Spoto, S. Bordiga, J.G. Vitillo, G. Ricchiardi, A. Zecchina, Stud. Surf. Sci. Catal. 155 (2005) 481.
[21] A. Züttel, Naturwissenschaften 91 (2004) 157.
[22] Ch. Wöll, J. Phys. Condens. Matter 16 (2004) S2981.
[23] J.B.L. Martins, J. Andrés, E. Longo, C.A. Taft, Int. J. Quant. Chem. 57 (1996) 861.
[24] M. Kunat, U. Burghaus, Ch. Wöll, Phys. Chem. Chem. Phys. 5 (2003) 4962.
[25] C.C. Chang, R.J. Kokes, J. Am. Chem. Soc. 93 (1971) 7107.
[26] R.J. Kokes, A.L. Dent, C.C. Chang, J. Am. Chem. Soc. 94 (1972) 4429.
[27] A.L. Dent, R.J. Kokes, J. Phys. Chem. 73 (1969) 3772.
[28] T.S. Askgaard, J.K. Norskov, C.V. Ovesen, P. Stoltze, J. Catal. 156 (1995) 229.
[29] T. Genger, O. Hinrichsen, M. Muhler, Catal. Lett. 59 (1999) 137.
[30] P. Li, Y. Wei, H. Liu, X. Wang, Chem. Commun. 24 (2004) 2856.
[31] D. Scarano, G. Spoto, S. Bordiga, A. Zecchina, C. Lamberti, Surf. Sci. 276 (1992) 281.
[32] D. Scarano, G. Ricchiardi, S. Bordiga, P. Galletto, C. Lamberti, G. Spoto, A. Zecchina, Faraday Discuss. 105 (1996) 119.
[33] F. Li, Y. Ding, P. Gao, X. Xin, Z.L. Wang, Angew. Chem. 116 (2004) 5350.
[34] P. Li, Y. Wei, H. Liu, X.J. Wang, Solid State Chem. 178 (2005) 855.
[35] T. Kawai, H. Kamio, T. Kondo, K. Kon-No, J. Phys. Chem. B 109 (2005) 4497.
[36] Z.R. Tian, J.A. Voigt, J. Liu, B. Mckenzie, M.J. Mcdermott, M.A. Rodriguez, H. Konishi, H. Xu, Nat. Mater. 2 (2003) 821.
[37] P.D. Cozzoli, M.L. Curri, A. Agostiano, G. Leo, M.J. Lomascolo, J. Chem. Phys. B 107 (2003) 4756.